

Copyright: ©2003 by WPMC Steering Board

Copyright and reproduction permission: All rights are reserved and no part of this publication may be reproduced or transmitted in any form or by any means, electronic or mechanical, including photocopy, recording, or any information storage and retrieval system, without permission in writing from the publisher. Notwithstanding, instructors are permitted to photocopy isolated articles for noncommercial classroom use without fee.

# Deficiencies of a Popular Stochastic MIMO Radio Channel Model

Ernst Bonek<sup>1</sup>, Hüseyin Özcelik<sup>1</sup>, Markus Herdin<sup>1</sup>, Werner Weichselberger<sup>1</sup> and Jon Wallace<sup>2</sup>  
{ernst.bonek, huseyin.ozcelik, markus.herdin, werner.weichselberger}@nt.tuwien.ac.at  
wall@ieee.org

<sup>1</sup>Institut für Nachrichtentechnik und Hochfrequenztechnik, Technische Universität Wien  
Gußhausstrasse 25/389, A-1040 Wien, Austria

<sup>2</sup>Department of Electrical and Computer Engineering, Brigham Young University  
Provo, UT 84602-4099, USA

## Abstract

Making a detailed review of the 'Kronecker' MIMO radio channel model we present important implications and deficiencies of this channel model. We show that the Kronecker model does not render the multipath structure correctly, but it introduces artifact paths that are not present in the underlying measurement data. Moreover, the Kronecker model underestimates the mutual information of the MIMO channel systematically which we demonstrate by analyzing measurement data of an  $8 \times 8$  MIMO system in indoor non-line-of-sight scenarios.

## 1 Introduction

Multiple-input multiple-output (MIMO) systems promise large information-theoretic capacities [1], enabling high data rate transmission, especially in rich multipath indoor scenarios. However, to develop such systems, it is essential to have an accurate description of the underlying channel. An important parameter of MIMO channels is the correlation between the channel matrix elements because correlation is known to significantly influence the capacity/mutual information. A well-known stochastic MIMO radio channel model that creates channel realizations based on correlations is the so-called 'Kronecker' model [2] [3], also known as IST-METRA model. This model was already investigated in several publications, e.g. McNamara et al. in [4] or [5], where the performance of the model was found to be satisfactory.

However, we show that this model does not render the multipath structure correctly, but it introduces artifact paths that are not present in the underlying measurement data and that therefore the mutual information estimated from this model is systematically below the mutual information of the measured channel.

The paper is organized as follows: Section 2 presents a review of the Kronecker model, stating the assumptions,

the implications and the deficiencies of the model. Section 3 briefly explains the measurement environment and the measurements we used to investigate the Kronecker model and Section 4 shows the results of the measurement evaluation, finally followed by Section 5 where we present some conclusions.

## 2 Review of the Kronecker Model

### 2.1 Signal Model and Notation

We consider in the following frequency-flat fading MIMO channels with  $m$  transmit and  $n$  receive antennas where each single realization of the channel can be described by the  $(n \times m)$  channel matrix  $\mathbf{H}$ . The received signal vector is given by

$$\mathbf{y} = \mathbf{H}\mathbf{x} + \mathbf{n} \quad (1)$$

where  $\mathbf{x}$  denotes the transmit signal vector and  $\mathbf{n}$  the noise at the receiver. The entries of the channel matrix  $\mathbf{H}$  are denoted by  $h_{ik}$ . Here, we will neglect the noise for the sake of simplicity.

In the following,  $\text{vec}\{\bullet\}$  denotes the vector operator stacking all elements of a matrix column-wise into a single vector,  $(\bullet)^T$  means transpose,  $(\bullet)^*$  complex conjugate,  $(\bullet)^H$  Hermitian transpose and  $E\{\bullet\}$  denotes the expectation operator. For an element-wise matrix notation we use  $\mathbf{A} = (a_{ij})$  which means that  $\mathbf{A}$  is build up from the elements  $a_{ij}$ . Furthermore, we use a matrix square root  $(\bullet)^{1/2}$  which fulfills  $(\bullet)^{1/2} \cdot ((\bullet)^{1/2})^H = (\bullet)$  and the Kronecker product denoted by  $\otimes$ .

### 2.2 Derivation of the Kronecker Model

In [2] and [3], a popular stochastic MIMO radio channel model was presented that allows the generation of MIMO channel realizations based on the receive and transmit correlation matrix. The basic idea, in slightly different

notation, is to generate a correlated Rayleigh fading channel matrix  $\tilde{\mathbf{H}} \in \mathbb{C}^{n \times m}$  according to

$$\text{vec}\{\tilde{\mathbf{H}}\} = \mathbf{R}_H^{1/2} \text{vec}\{\mathbf{G}\} \quad (2)$$

where

$$\mathbf{R}_H = E\{\text{vec}\{\mathbf{H}\}\text{vec}\{\mathbf{H}\}^H\} \quad (3)$$

is the  $(nm) \times (nm)$  channel correlation matrix containing the complex correlation between all  $(nm)$  elements of the  $(n \times m)$  channel matrix  $\mathbf{H}$ .  $\mathbf{G}$  is a random fading matrix with unity power independent entries determining the single element fading statistics of  $\mathbf{H}$ . In case of Rayleigh fading, it has zero-mean i.i.d. complex Gaussian entries with unity variance. Note that for a Rayleigh fading channel, the second order statistics  $\mathbf{R}_H$  contains the full channel knowledge.

There are two assumptions necessary and sufficient for a Kronecker structure of the full channel correlation matrix:

- (I) The receive antenna correlation between any pair of receive antennas  $(i, j)$  given by

$$\rho_{R_x,ij}(k) = E\{h_{ik}h_{jk}^*\} \quad (4)$$

has to be independent of the transmit antenna  $k$ . In matrix notation we can now define the receive correlation matrix by

$$\mathbf{R}_{R_x} = E\{\mathbf{H}\mathbf{H}^H\} = m \cdot (\rho_{R_x,ij}). \quad (5)$$

Analogously, the transmit antenna correlation between each transmit antenna pair  $(k, l)$  given by

$$\rho_{T_x,kl}(i) = E\{h_{ik}h_{il}^*\} \quad (6)$$

has to be independent of the receive antenna  $i$ . In matrix notation we can now define the transmit correlation matrix by

$$\mathbf{R}_{T_x} = E\{\mathbf{H}^T\mathbf{H}^*\} = n \cdot (\rho_{T_x,kl}) \quad (7)$$

This leads to equal power  $P_h = E\{|h_{ik}|^2\}$  of all channel matrix elements.

- (II) The correlation coefficient between any pair of channel matrix elements, as given by the full channel correlation matrix  $\mathbf{R}_H$ , has to be the product of the corresponding receive and transmit antenna correlation coefficient normalized by the power of one channel matrix element:

$$\rho_{H,ik,jl} = E\{h_{ik}h_{jl}^*\} = \frac{1}{P_h} \cdot \rho_{R_x,ij} \cdot \rho_{T_x,kl} \quad (8)$$

This can be equivalently formulated in matrix notation with  $\text{tr}\{\mathbf{R}_{R_x}\} = \text{tr}\{\mathbf{R}_{T_x}\} = m \cdot n \cdot P_h$ :

$$\mathbf{R}_H = \frac{1}{\text{tr}\{\mathbf{R}_{R_x}\}} \mathbf{R}_{T_x} \otimes \mathbf{R}_{R_x}. \quad (9)$$

With these assumptions and the identities

$$[\mathbf{B}^T \otimes \mathbf{A}]\text{vec}\{\mathbf{D}\} = \text{vec}\{\mathbf{ADB}\} \quad (10)$$

$$(\mathbf{A} \otimes \mathbf{B})(\mathbf{C} \otimes \mathbf{D}) = (\mathbf{AC}) \otimes (\mathbf{BD}), \quad (11)$$

equation (2) simplifies to the so-called ‘Kronecker’ model

$$\tilde{\mathbf{H}} = \frac{1}{\sqrt{\text{tr}\{\mathbf{R}_{R_x}\}}} \mathbf{R}_{R_x}^{1/2} \mathbf{G} (\mathbf{R}_{T_x}^{1/2})^T. \quad (12)$$

Beside simplified analytical treatment or simulation of MIMO systems, (12) allows for independent array optimization at Tx and Rx. Therefore, and because of the simplicity of this approach, the Kronecker model has become popular.

### 2.3 Implications of the Kronecker Assumption

To consider the effect of the Kronecker assumption on the directions of arrival (DOAs) and directions of departure (DODs), we have to look at the structure of the receive and transmit correlation matrix for different transmit and receive weights, respectively. Using (12), the receive correlation matrix  $\mathbf{R}_{R_x,w}$  for beamforming at Tx side, i.e. using specific transmit weights  $\mathbf{w}$  is given by

$$\mathbf{R}_{R_x,w} = E\{\mathbf{H}\mathbf{w}\mathbf{w}^H\mathbf{H}^H\} = \frac{1}{\text{tr}\{\mathbf{R}_{R_x}\}} \cdot$$

$$E\left\{ \mathbf{R}_{R_x}^{1/2} \mathbf{G} \underbrace{\left( \mathbf{R}_{T_x}^{1/2} \right)^T \mathbf{w} \mathbf{w}^H \left( \mathbf{R}_{T_x}^{1/2} \right)^*}_{\mathbf{X}} \mathbf{G}^H \left( \mathbf{R}_{R_x}^{1/2} \right)^H \right\}.$$

(13)

where we use  $\mathbf{X}$  as an abbreviation for the inner part. It is straight-forward to show that  $E\{\mathbf{GXG}^H\}$  is always an identity matrix scaled by a complex scalar factor  $K$ , if  $\mathbf{G}$  is a unity power, independently distributed complex Gaussian random matrix (see Appendix). Therefore the receive correlation matrix  $\mathbf{R}_{R_x,w}$  for the transmit weights  $\mathbf{w}$  is equal to

$$\mathbf{R}_{\text{Rx},w} = \frac{1}{\text{tr}\{\mathbf{R}_{\text{Rx}}\}} \mathbf{R}_{\text{Rx}}^{1/2} \mathbf{K} \mathbf{I} \left( \mathbf{R}_{\text{Rx}}^{1/2} \right)^H = K' \cdot \mathbf{R}_{\text{Rx}} \quad (14)$$

This means that the structure of the receive correlation matrix does not change if we use different transmit weights, the receive correlation matrix is only scaled by a complex constant. Using for example a beamforming vector to transmit to a specific direction leads always to a scaled version of the same receive correlation matrix and, therefore, to a scaled version of the same DOA profile. This holds also true for the transmit correlation matrix and the corresponding DODs.

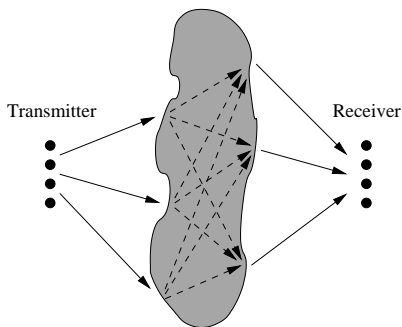


Figure 1: The Kronecker model enforces that all directions of departure are linked to all directions of arrival, the joint DOA-DOD spectrum of a Kronecker synthesized channel is the product of the average DOA and the average DOD spectrum

Considering the joint DOD-DOA spectrum we can therefore say that the Kronecker model enforces it to be the product of the DOD and the DOA spectrum. In other words (as illustrated in Figure 1), this means that all directions of departure are linked to all directions of arrival, only the total power of the DOAs depends on the chosen DOD, analogously only the total power of the DODs depends on the chosen DOA.

#### 2.4 Physical Interpretation of the Kronecker Assumption

A physical interpretation of the Kronecker assumption is this: Irrespective of which transmit weight vector is chosen, the scatterers surrounding the receiver are illuminated by one and the same power distribution. Therefore, the same DOA spectrum is generated. The same DOA spectrum means identical receive correlation. The total receive power may, of course, vary.

Any arbitrary transmit weight vector does include the case of a single antenna transmitting, which is assumption (I) in our paper. Other than stated in [3] and other papers, this condition alone is not sufficient. The same holds true for the reverse link.

## 2.5 Deficiencies of the Kronecker Model

The main deficiency of the Kronecker model is that the multipath structure of the synthesized channel is significantly different to the multipath structure of the underlying measured channel. Whereas it is very likely that single DODs are linked to single DOAs, the Kronecker model enforces, as shown before, the synthesized channel to be such that every DOD couples into every DOA by enforcing the joint DOD-DOA spectrum to be the product of the DOD and the DOA spectrum.

This modification of the multipath structure leads to lower mutual information estimates when using the synthesized channels than when using the measurement data directly. Instead, the diversity of the channel is increased. We will show the mutual information mismatch by using measurement data in the results section. An explanation for this behavior can be found in [6].

## 3 Measurement

### 3.1 Measurement Setup

For the measurements, we used the wideband vector channel sounder RUSK ATM [7] with a measurement bandwidth of 120 MHz at a center frequency of 5.2 GHz. At the transmit (Tx) side, a monopole antenna was mounted on a 2D positioning table forming a  $\lambda/2$  spaced virtual array of  $20 \times 10$  positions, where we used only a  $10 \times 5$  submatrix for the evaluation to keep clear of large-scale effects. The receiver (Rx) was a directional 8-element uniform linear array (ULA) with  $0.4\lambda$  inter-element spacing and two additional dummy elements. The antenna elements were printed dipoles with a backplane having  $120^\circ$  3dB beamwidth.

For each Tx position the channel sounder measured 128 temporal snapshots of the frequency dependent transfer function between the Tx monopole and all Rx antennas. Within the measurement bandwidth of 120MHz, 193 equidistant frequency samples of the channel coefficients were taken giving a 4-dimensional complex channel transfer matrix (snapshot, frequency, Rx and Tx position). Since the measurement of the whole 4-dimensional channel transfer matrix took about 10 minutes, we measured at night to ensure stationarity.

### 3.2 Environment

The measurements were carried out in the offices of the *Institut für Nachrichtentechnik und Hochfrequenztechnik, Technische Universität Wien*. In total, 24 Rx positions were measured: one in a hallway - with line-of-sight (LOS) to Tx, 23 of them in several office rooms connected to this hallway - with non-line-of-sight (NLOS) to Tx. The (virtual) Tx array was always positioned in the same place in the hallway. Some rooms were amply, others sparsely furnished with wooden and metal furniture

and plants. At each position, we rotated the Rx antenna to three different broadside directions D1, D2 and D3 that were angularly spaced by 120°. Thereby, we get 72 different 'scenarios', i.e. combinations of Rx positions and directions.

### 3.3 Evaluation

For each Rx position and direction we created 15 spatial realizations of the  $8 \times 8$  MIMO channel matrix by moving a virtual 8-element uniform linear array (ULA) over the  $10 \times 5$  Tx grid. Taking the 193 frequency bins, the total set of channel samples is formed by  $193 \cdot 15 = 2895$  different spatial and frequency realizations. Considering a channel unknown at Tx, the mutual information of the MIMO channel for each realization was calculated by [1]

$$C = \log_2 \det(\mathbf{I}_m + \frac{\rho}{n} \mathbf{H}\mathbf{H}^H) \quad (15)$$

where  $\mathbf{I}_m$  denotes the  $m \times m$  unity matrix,  $\rho$  the mean receive SNR,  $n$  the number of Tx antennas and  $\mathbf{H}$  the normalized  $m \times n$  MIMO channel matrix. Here,  $m = n = 8$ . The normalization was done such that the average receive SNR for each scenario was 20dB [8]. Additionally, we synthesized  $193 \cdot 15 = 2895$  different realizations of  $\tilde{\mathbf{H}}$  according to the 'Kronecker' model (12), normalized them and compared the resulting mutual information for both measured and 'Kronecker' model channel matrices.

## 4 Results

In Figure 2, the *average* mutual information when using the 'Kronecker' model vs the *average* mutual information estimated directly from the measurement data for each scenario is shown. As can be seen, the 'Kronecker' model always underestimates the true mutual information, i.e. the points lie below the identity (dashed) line. The dash-dotted and dashed lines correspond to 10% and 20% relative error, respectively.

Moreover, the mismatch in mutual information gets worse with decreasing 'measured' mutual information. Since decreasing 'measured' mutual information is related to increasing correlation at either or both receive and transmit sides [9] [8], it shows that the 'Kronecker' model fails in correlated environments.

Why is 'Kronecker' mutual information always lower than that one estimated directly from the measurement? Figure 3 provides a compelling answer by comparing the joint DOD-DOA Fourier spectrum of a typical scenario for measured channels (top) and channels synthesized with the 'Kronecker' model (bottom). In the measured channel, specific DODs are clearly linked to specific DOAs, such that the joint spectra is not separable into a product of the DOD and the DOA spectrum. The

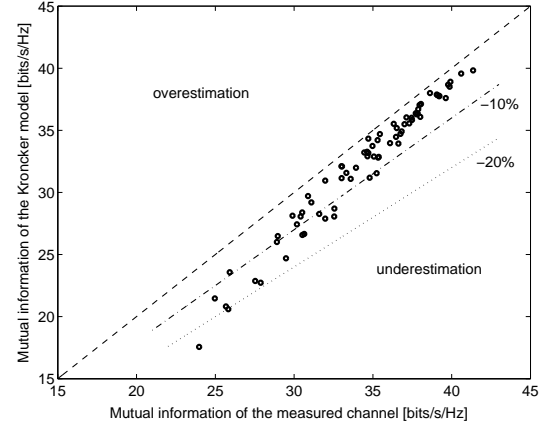


Figure 2: Average mutual information of 'Kronecker' model generated and measured channel for an  $8 \times 8$  MIMO system for 72 different scenarios

Kronecker factorization, however, forces the joint spectrum to be separable, thus introducing artifact paths lying at the intersections of DOD and DOA spectral peaks. As explained in [6], these artifacts lower average mutual information but increase diversity order. These effects will likely be more pronounced for large arrays with high angular resolution.

## 5 Conclusion

We reviewed the 'Kronecker' MIMO radio channel model and considered the assumptions, the implications and the deficiencies that the factorization into separated receive and transmit correlation matrices causes. We showed that the Kronecker assumption forces the joint DOD-DOA spectrum of the channel model to be the product of the DOA and the DOD spectrum and therefore enforces that each DOD is linked to each DOA. However, in reality, as we show with measurements, it is likely to happen that single DODs are linked to single DOAs, which the model is not able to reproduce.

Additionally, the mutual information predicted by the 'Kronecker' model is always below the mutual information estimated from the measured channel directly. By analyzing a large set of broadband indoor measurements, we found a capacity mismatch, which increases with increasing correlation, of up to 27% for an assumed average receive SNR of 20dB. The reason for this is again incorrect reproduction of the multipath structure, which introduces artifact paths in the joint DOD-DOA spectrum, resulting necessarily in lower capacity but higher diversity. Note that our results are not in contradiction to [5], where the authors claimed to have validated 'Kronecker' factorization and modeling for a  $2 \times 2$  and  $3 \times 3$  system, since these deficiencies are not so pronounced because of the reduced spatial resolution of their systems.

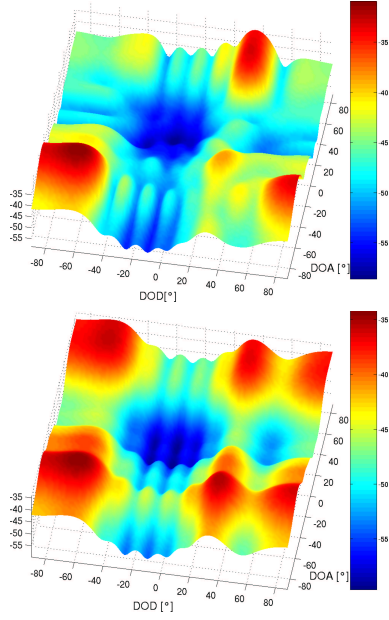


Figure 3: Joint DOD-DOA Fourier spectrum (in dB) of the measured channel matrix (top) and of the Kronecker model (bottom) - example scenario

## Acknowledgment

We would like to thank Helmut Hofstetter (ftw.) for help with the measurements and T-Systems Nova GmbH for providing an eight element uniform linear array of printed dipoles.

## Appendix

Let  $\mathbf{G}$  be a  $(n \times m)$  complex Gaussian random matrix with unity power and independently distributed elements  $g_{ij}$ . For such a matrix

$$\mathbf{Y} = E\{\mathbf{G}\mathbf{X}\mathbf{G}^H\} \quad (16)$$

is always equal to a scaled identity matrix  $K \cdot \mathbf{I}_n$ . Writing the matrix multiplication element-wise, the elements of  $\mathbf{Y}$  become

$$y_{ij} = E\left\{\sum_{k=1}^m g_{ik} \sum_{l=1}^m x_{kl} g_{jl}^*\right\} = \sum_{k=1}^m \sum_{l=1}^m E\{g_{ik} x_{kl} g_{jl}^*\}. \quad (17)$$

Since the elements of  $\mathbf{G}$  are independent and identically distributed, the expectation of the right hand side of (17) is non-zero only for  $i = j$  and  $k = l$ , and therefore (17) simplifies to

$$y_{ij} = \begin{cases} E\left\{\sum_{k=1}^m |g_{ik}|^2 \cdot x_{kk}\right\} & i = j \\ 0 & i \neq j \end{cases} \quad (18)$$

Or equivalently with  $P_g = E\{|g_{ik}|^2\}$

$$\mathbf{Y} = \left(P_g \cdot \sum_{k=1}^m x_{kk}\right) \cdot \mathbf{I}_n \quad (19)$$

## References

- [1] I.E. Telatar, "Capacity of multi-antenna gaussian channels," *AT&T Bell Labs*, online available: <http://mars.bell-labs.com/cm/ms/what/mars/papers/proof>.
- [2] K.I. Pedersen, J.B. Andersen, J.P. Kermoal, and P. Mogensen, "A stochastic multiple-input-multiple-output radio channel model for evaluation of space-time coding algorithms," *IEEE VTC Fall 2000*, Sept. 2000.
- [3] J.P. Kermoal, L. Schumacher, K.I. Pedersen, P.E. Mogensen, and F. Frederiksen, "A stochastic MIMO radio channel model with experimental validation," *IEEE Journal on Selected Areas in Communications*, vol. 20, pp. 1211–1226, Aug. 2002.
- [4] D.P. McNamara, M.A. Beach, and P.N. Fletcher, "Spatial correlation in indoor MIMO channels," *Personal Indoor and Mobile Radio Communications*, vol. 1, pp. 290–294, 2002.
- [5] K. Yu, M. Bengtsson, B. Ottersten, D. McNamara, P. Karlsson, and M. Beach, "Second order statistics of NLOS indoor MIMO channels based on 5.2 GHz measurements," *IEEE Globecom 2001*, vol. 1, pp. 156–160.
- [6] A.M. Sayeed, "Deconstructing multiantenna fading channels," *IEEE Transactions on Signal Processing*, vol. 50, pp. 2563–2579, Oct. 2002.
- [7] R.S. Thomä, D. Hampicke, A. Richter, G. Sommerkorn, A. Schneider, U. Trautwein, and W. Wornitz, "Identification of time-variant directional mobile radio channels," *IEEE Transactions on Instrumentation and Measurement*, vol. 49, pp. 357–364, April 2000.
- [8] H. Özcelik, M. Herdin, H. Hofstetter, and E. Bonek, "A comparison of measured  $8 \times 8$  MIMO systems with a popular stochastic channel model at 5.2 GHz," *ICT*, vol. 2, pp. 1542–1546, 2003.
- [9] D.S. Shui, G.J. Foschini, M.J. Gans, and J.M. Kahn, "Fading correlation and its effect on the capacity of multielement antenna systems," *IEEE Transactions on Communications*, vol. 48, no. 3, pp. 502–513, March 2000.